Published in final edited form as:
J Nucl Med. 2012 September ; 53(9): 1392–1400. doi:10.2967/jnumed.111.100909.

Direct Quantification of Post-Stress-Rest Left Ventricular Motion and Thickening Changes for Myocardial Perfusion SPECT

Shahryar Karimi-Ashtiani[1], **Reza Arsanjani**[1], **Mathews Fish**[3], **Paul Kavanagh**[1], **Guido Germano**[1,2], **Daniel Berman**[1], and **Piotr Slomka**[1,2]

[1]Departments of Imaging and Medicine, and Cedars-Sinai Heart Institute, Cedars-Sinai Medical Center, Los Angeles, CA

[2]David Geffen School of Medicine, University of California Los, Los Angeles, CA

[3]Oregon Heart and Vascular Institute, Sacred Heart Medical Center, Springfield, OR

Abstract

Changes in myocardial wall motion and thickening during myocardial perfusion single-photon emission computed tomography (MPS) are typically assessed separately from gated studies to assess for stress induced functional abnormalities. We sought to develop and validate a novel approach for automatic quantification of post-stress-rest myocardial motion and thickening changes (MTC).

Methods—Endocardial surfaces at the end-diastolic and end-systolic frames for post-stress and rest studies were registered automatically to each other by matching ventricular surfaces. Myocardial MTCs were computed and normal limits of change were determined as the mean and standard deviation for each polar sample. Normal limits were utilized to quantify the MTCs for each map and the accumulated sample values were used for abnormality assessments in segmental regions. A hybrid method was devised by combining the Total Perfusion Deficit (TPD) and MTC for each vessel territory. Normal limits were obtained from 100 subjects with low likelihood (LLK) of coronary artery disease (CAD). For validation, 623 subjects with correlating invasive angiography were studied. All subjects had a stress/rest ^{99m}Tc-sestamibi exercise or adenosine test, and all had coronary angiography within 3 months of MPS. All MTC and TPD measurements were derived automatically. The diagnostic accuracy for detection of coronary artery disease for MTC+TPD was compared to TPD alone.

Results—Segmental normal values for motion change were between −1.3 and −4.1 mm and between −30.1% and −9.8% for thickening change. MTC combined with TPD achieved 61% sensitivity for 3-vessel disease (3VD), 63% for 2-vessel disease (2VD), and 90% for 1-vessel disease (1VD) detection vs. 32% for 3VD ($P < 0.0001$), 53% for 2VD ($P < 0.001$), and 90% for 1VD ($P = 1.0$) detection with TPD alone method. The specificity for the combined method was 71% for 3VD, 72% for 2VD, and 47% for 1 VD detection vs. 90% for 3VD ($P < 0.0001$), 80% for 2VD ($P < 0.001$), and 50% for 1VD detection ($P=0.0625$) for TPD alone method. The accuracy of 3VD detection by MTC+TPD was higher (69%) than the accuracy of TPD + change in ejection fraction (63%), ($P< 0.004$).

Corresponding Author Info: Piotr J. Slomka, PhD, Artificial Intelligence in Medicine Program, 8700 Beverly Blvd, Ste #A047, Los Angeles, CA 90048, USA, Ph: 310-423-4348, piotr.slomka@cshs.org.
First Author Info: Shahryar Karimi-Ashtiani, PhD (Post-doctoral fellow), Cedars-Sinai Medical Center, 8700 Beverly Blvd, Taper #A238, Los Angeles, CA 90048, USA, Ph: 310-423-8705, shahryar.karimi@gmail.com

All others disclose no current conflict of interest.

Conclusion—We established normal limits and a novel method for computation of regional functional changes between post-stress and rest. Combination of (TPD) with MTC improved the sensitivity for the detection of 3VD and 2VD as compared to TPD alone.

Keywords

Surface registration; Motion; Thickening; 3 vessel disease; Coronary artery disease; SPECT

Myocardial perfusion single photon emission computed tomography (MPS) is the most widely employed diagnostic test for detection of coronary artery disease (CAD) (1, 2). Abnormalities in myocardial perfusion and function during stress, which were not present during the rest study, often signify impaired perfusion reserve, and are strong markers for existence of high-grade stenosis and ischemia. Traditionally, global perfusion measures such as summed stress and rest scores (SSS/SRS) (3), total perfusion deficit (TPD) (4), or summed stress-rest perfusion changes (5) have been used for detection of CAD. However, certain conditions such as severe CAD in patients with three-vessel disease (3VD) pose technical and diagnostic challenges (5, 6). Additional functional data, such as measurements of ejection fraction (EF) and its changes between the post-stress and rest studies, can be utilized to improve the detection of CAD (7).

It has previously been shown that reversible regional wall motion abnormality following stress, which was not present during rest, is a strong predictor of angiographic severity and adds incremental value to the perfusion data in assessment of severity (8, 9). The standard method of analysis for motion and thickening, however, may suffer from variability in contour placements when subtle changes in motion and thickening are being evaluated. We aimed to evaluate quantitatively regional myocardial motion and thickening changes (MTC) between post-stress and rest studies using a novel myocardial surface registration method. Furthermore, we investigated whether these derived functional measurements provide any incremental improvement for diagnosis of multi-vessel coronary disease, as compared to information provided by perfusion data alone.

MATERIALS AND METHODS

Patient Population

This was a retrospective cohort study and all the cases were selected consecutively. Institutional Review Board approval was obtained for anonymous review of the data. The total study population consisted of 723 patients who underwent exercise or adenosine stress ^{99m}Tc-sestamibi MPS. The studies were performed using standard ^{99m}Tc-sestamibi rest/stress protocols. We established normal limits from a group of 100 patients (70 women, 30 men) with a LLK of CAD (<5%) (training group) who were selected consecutively on the basis of age, sex, pretest symptoms, and electrocardiogram response to adequate treadmill stress testing. The selection of these normal subjects was based on the Diamond and Forrester criteria (10). Angiographic validation was obtained using 623 consecutive patients (353 men, 270 women) who had coronary angiography within 3 months of MPS. Exclusion criteria were as follows: prior myocardial infarction or coronary revascularization, nonischemic cardiomyopathy or vascular heart disease, and change in symptoms between MPS and coronary angiography. To examine the performance of the MTC method for incremental value in multi-vessel detection, a mixed population of patients consisting of 176 cases with 0-vessel, 197 cases with 1-vessel, 141 cases with 2-vessel, and 109 cases with 3-vessel CAD were selected (CAD group). All 623 cases in this group underwent coronary angiography tests within three months of their SPECT scans and none of the patients had any cardiac events during this period. The results of angiography were treated as the gold standard for validation of other methods. The majority of normal training cases contained 8-

bin gated SPECT studies (98 out of 100 cases). The SPECT data constituting the CAD group was a mixture of 8 and 16 gated SPECT. For the stress studies, the patients underwent only exercise SPECT in the LLK groups; however, 417 out of 623 cases in the CAD group underwent adenosine SPECT. The detailed baseline characteristics for LLK and CAD group are summarized in Table 1.

Statistical Analysis

Continuous variables were expressed as the means ± standard deviation, and categorical variables were expressed as percentages (%). Comparison of sensitivity and specificity between groups were made using McNemar's test. For all analyses, P values <0.05 were considered statistically significant.

Image Acquisition and Reconstruction and Left ventricular segmentation

The details of image acquisition and tomographic reconstruction have been previously described (11–13). In brief, studies were performed by using standard ^{99m}Tc-sestamibi rest/stress protocols. All subjects were imaged at 60 min after the administration of ^{99m}Tc-Sestamibi at rest followed by stress images taken at 15–45 min after either radiopharmaceutical injection during treadmill testing or adenosine infusion with low-level exercise. Data were acquired on Vertex, dual-detector scintillation camera with low energy high-resolution collimators (Philips Medical Systems, Milpitas, CA). Vantage Pro attenuation correction transmission images were also collected, but were not used for the reconstruction of the gated data or any analysis in this study. The system SPECT resolution for this type of camera with high resolution collimators and FBP reconstruction is approximately 10 mm.

Tomographic reconstruction was performed by use of the AutoSPECT (Philips Medical Systems) for both gated and un-gated studies. The alignment of the projection data to the reconstruction matrix was applied to determine the mechanical center of rotation. Butterworth filters were applied to obtain the non-corrected MPS with an order of 10 and cutoff of 0.50 for rest MPS, and an order of 5 and cutoff of 0.66 for stress MPS. Scatter correction was also incorporated into this reconstruction, along with non-stationary, depth-dependent resolution compensation. The short-axis reconstruction angles were automatically determined by the software.

Quality control was performed on all gated images including reviewing of the ECG rhythm strip to exclude any significant arrhythmia, visual review of the cine gated images with special emphasis placed on end-diastolic images, and reviewing of the time volume curve. Contours were automatically extracted with QGS algorithm, as previously described (14), separately for stress and rest gated short-axis images and also for stress and rest perfusion images for the calculation of TPD. The automatically extracted contours were verified by an expert technologist with manual adjustment needed in approximately 25% of the angiographic cases and 12% of LLK cases. All further image processing tasks, including quantification of perfusion and TPD, were performed automatically and were incorporated into the software tool for cardiac quantification developed at our institution (15)

Conventional Coronary Angiography

Conventional coronary angiography was performed according to standard clinical protocols within 3 months of the myocardial perfusion examination. All coronary angiograms were visually interpreted by an experienced cardiologist. A stenosis of 50% or greater narrowing of luminal diameter of the left main or 70% or greater narrowing of the other vessels was considered significant and was used as the gold standard for the detection of CAD.

Myocardial Surface Registration

For representation of myocardial surface points, the best ellipsoid fit was utilized for left ventricle (LV) segmentation (14) shown in Figure 1. Segmentations of myocardium by best ellipsoid fits are performed independently at ED and ES frames, which could lead to a disparity between the actual physical locations, on the two surfaces. Therefore, a point represented by (a, p) coordinates on the ED ellipsoid may actually map onto different (a', p') coordinates, which is a point represented on the ES ellipsoid, as shown in Figure 1. Attempts at resolving this registration problem involve a number of practical challenges. It should be noted that myocardium appears brighter at ES relative to the ED image, which is the result of myocardial wall thickening at ES and the partial volume effect. In order to address this problem, we normalized each image data to its 85% maximal count percentile, bringing all data samples to the similar intensity range. We then defined the sum of absolute intensity differences (SAD) to measure the global degree of disparity between the indexing systems at different phases;

$$\mathrm{SAD}_{\mathrm{ED,ES}} = \sum_{a,p} [\alpha \{I_{\mathrm{ED}}(a, p) - I_{\mathrm{ES}}(a, p)\} + \beta \{\nabla I_{\mathrm{ED}}(a, p) - \nabla I_{\mathrm{ES}}(a, p)\}] \quad (1)$$

where I_{ED} and I_{ES} are the intensity (after count normalization) at ED and ES times, ∇ is the gradient operator, and $0 \leq \alpha, \beta \leq 1$. For the experiments in this study, the values of α and β were empirically set to 0.1 and 0.9, respectively. The gradient term was intentionally given more weight, since the magnitude of the gradient term in contour regions is typically one order of magnitude smaller than intensity, β was chosen to be one order of magnitude larger.

The minimal $\mathrm{SAD}_{\mathrm{ED,\ ES}}$ is achieved when there is an exact one-to-one mapping between the two indexing systems (i.e. a=a' and b=b') and the two surfaces are perfectly registered. The disparities between indexed points of two ellipsoids can be alleviated by minimizing $\mathrm{SAD}_{\mathrm{ED,ES}}$ by 3D rotation of one of the ellipsoids (while the included LV is stationary). Therefore, minimizing $\mathrm{SAD}_{\mathrm{ED,\ ES}}$ is equivalent to finding the best indexing set, which registers the two myocardial surfaces. The optimal rotation around each axis was achieved by performing a search in 3 degree steps.

An analogous approach was also used for mapping myocardial surfaces between post-stress and rest studies for MTC computation (See Figure 2). Registration is achieved by finding the optimal rotation that results in the minimal SAD function between post-stress and rest studies, which is defined as;

$$\mathrm{SAD}_{\mathrm{S\_ED,R\_ES}} = \sum_{a,p} [\alpha \{I_{\mathrm{S\_ED}}(a, p) - I_{\mathrm{R\_ES}}(a, p)\} + \beta \{\nabla I_{\mathrm{S\_ED}}(a, p) - \nabla I_{\mathrm{R\_ES}}(a, p)\}] \quad (2)$$

where I_{S_ED} and I_{R_ES} are the intensity of the images for post-stress study at ED, and rest study at ES times, respectively. Minimization of equation (2) is equivalent to registering the ED surface of the post-stress study to ES surface of rest study, with the valve plane location being copied from the post-stress to the rest.

Stress-Rest Motion and Thickening Changes

For any point on a myocardial surface, the motion was defined as the absolute displacement of the point during ED to ES interval, and thickening was defined as the absolute distance between epicardial and endocardial walls. The post-stress-rest motion change for a polar map sample was defined as the difference between motion values of the sample in post-stress and rest studies, while myocardial wall thickening was defined as the percentage of wall thickness increase between the ED to ES time frames. After registering the endocardial surfaces for every polar map sample, the post-stress-rest motion changes were computed. In

addition, post-stress-rest thickening changes were defined as the difference between wall thickening at post-stress and rest studies, which was defined for every polar map sample. These values were regionally averaged based on the 17-segment model. For each segment, the mean and standard deviations were calculated utilizing the training set population.

Normal Limits and Automatic Abnormality Detection

From the training population, two sets of normal limits were estimated for post-stress-rest motion and thickening changes. For each set, we calculated the normal limits for every polar map sample by estimating the sample mean and standard deviation derived from the training set.

In order to quantify these abnormalities in MTC, we considered values within the 2-standard-deviation below the mean as the normal (non-ischemic) range for each polar map MTC signature. In order to measure the degree of abnormality, an *abnormality severity measure* was defined. For each polar map, a MTC measure received a *Severity Measure* of 0 if it was within the two-standard-deviation normal range. Similarly, the MTC measures between 2 and 3, 3 and 4, and beyond 4 standard deviations of the mean, were assigned *Severity Measures* of 1, 2, and 3 respectively.

Detection of CAD in Individual Vessels

For each functional signature (motion and thickening), the *Severity Measures* were computed at each polar map site and then were averaged over each vessel territory region; therefore, establishing the *regional MTC Severity*. Segmentation of the polar map into vessel territories (i.e., left anterior descending (LAD), left circumflex (LCX), and right coronary artery (RCA)) was performed automatically by Cedars-Sinai QPS/QGS software (15). Normal limits for a functional signature for regional MTCs derived by calculation of the mean and standard deviation over the training set. Two separate sets of regional normal limits were calculated for motion changes and for thickening changes.

MTC was added to the baseline TPD (16) and ischemic TPD (4) in order to evaluate its incremental effects on diagnosis of 1-vessel (1VD), 2-vessel (2VD) and 3VD. For each vascular territory, we ran two parallel diagnostic tests (motion change and thickening test) by using the corresponding regional normal limits. The outcomes of the two tests for each vessel territory were then combined by disjunction operator (Logical OR) to comprise *regional MTC Test.* The results of *regional* MTC *Test*s were used to complement the traditional regional stress TPD measure, as well as the regional ischemic TPD, establishing our proposed hybrid diagnostic method. Figure 3 illustrates this high level schematic for our proposed system for detection of 3VD.

The hybrid rule was devised to combine the outcomes of regional TPD and MTC with the intention of improving the sensitivity of TPD-only measures. A regional TPD of ≥ 2% in each coronary territory was considered abnormal for per-vessel analysis (12, 17, 18). For the hybrid method to be considered positive in a given vessel territory, either the TPD or MTC result was required to be positive in this territory.

RESULTS

The normal values for post-stress-rest motion change ranged between −1.3 and −4.1 mm, with the most significant motion change occurring in the apical region (−3.2 to −4.1 mm). The normal values for post-stress-rest thickening changes ranged between −30.1% to −9.8%, with the most substantial thickening changes occurring in the basal segments with the exception of basal anteroseptal region (−9.8%). Figure 4 illustrates the segmental normal limits for the post-stress-rest motion and thickening changes. The right column presents the

lower thresholds for normal range, and the values below these limits were considered abnormal.

The comparison of the sensitivity and specificity of perfusion data and our hybrid method for detection of 3VD is shown in Figure 5. The sensitivity and specificity of ischemic TPD was 21% and 95% respectively (5A), which agrees with prior studies (6). The addition of either motion or thickening change to the ischemic TPD provided incremental improvement in sensitivity; however, the addition of both resulted in further significant improvement in sensitivity (52%, $P < 0.0001$) with an expected decline in overall specificity (74%, $P < 0.0001$). The sensitivity and specificity of stress TPD were 32% and 90% respectively. The addition of motion and thickening each provided improvements in sensitivity and the addition of both resulted in further improvement in sensitivity (61%, $P < 0.0001$) and reduced specificity (71%, $P < 0.0001$). By utilizing our hybrid method, we were able to identify 32 more cases of out of 109 total patients with 3VD.

The comparison of the sensitivity and specificity of perfusion data and our hybrid method for detection of 1VD and 2VD is shown in Figure 6. The addition of MTC to the ischemic TPD once more provided incremental improvement in sensitivity; however addition of both resulted in significant improvement in sensitivity for detection of 2VD (63% vs. 53%, $P <0.001$), with subsequent decline in specificity (72% vs. 80%, $P <0.001$). There was no significant change in sensitivity (90% vs. 90%, $P = 1$) or specificity (47% vs. 50%, $P = 0.0625$) utilizing our hybrid method for detection of 1VD.

Furthermore, it has previously been shown that the global EF change between post-stress and rest studies provide incremental diagnostic value for detection of severe ischemic condition (7). The combination of the territorial stress TPD and the change in EF between the post-stress-rest studies (with ≥ 5% drop in EF following stress set as the abnormality threshold) resulted in overall 63% accuracy for detection of 3VD (19). By comparison, our hybrid method of combining stress TPD and MTC had a 69% accuracy ($P < 0.004$), which further shows the overall improvement in performance of our proposed method for detection of 3VD as compared to existing tools. It is, however, important to bear in mind that a drop in EF following stress is a global measure and not necessarily a specific marker for 3VD.

Figure 7 shows an example of how our hybrid method is able to provide incremental diagnostic value in addition to those provided by perfusion data. The patient underwent an exercise ^{99m}Tc-Sestamibi, the results of which are shown in Figure 7A. The patient's perfusion study clearly shows a reversible perfusion defect in anterior and lateral wall (left anterior descending and left circumflex territories); however, addition of MTC also demonstrated a motion abnormality in the RCA territory. Her angiogram confirmed the presence of severe 3 vessel obstructive coronary artery disease.

DISCUSSION

Diagnosis of multi-vessel CAD using MPS is associated with significant technical and clinical challenges. In patients with multi-vessel CAD, an overall global count deficiency in perfusion might exist. Based on the lack of normal landmarks during the count normalization process, this can lead to overall reduced discrepancies between the normal limits and the ischemic regions (20). As a result, these hypoperfused regions could appear as normal, resulting in decreased sensitivity of the test. This decrease in sensitivity can be quite significant with 20% of patients with 3VD having normal MPS scans and only about 29% of patients with 3VD having perfusion abnormalities in all 3 coronary territories (5, 6). This is unfortunate, because the patients with multi-vessel disease might benefit most from early detection and revascularization especially if they have compromised left ventricular function

(21, 22). In patients with severe CAD, the myocardium may exhibit compromised contractile function such as reduced wall motion and thickening, and prior studies have shown that supplementing either regional or global functional data from the electrocardiography-gated SPECT stress studies to the perfusion quantification improved the accuracy of multi-vessel disease detection (7, 20, 23).

Emmett and colleagues demonstrated in 2002 (8) that post-stress and reversible regional wall motion abnormality was a strong predictor of obstructive CAD and provided incremental diagnostic value to MPS for assessment of angiographic severity. In their study, reversible regional wall motion abnormality (RWMA) had 53% sensitivity and 100% specificity for identifying angiographic stenoses ≥ 70%. Furthermore, they noted that reversible RWMA as well as post-stress RWMA were strong predictors of angiographic severity. The overall advantage of our hybrid method is that by registering the myocardial surfaces, we are able to identify subtle changes between rest and post-stress, which might otherwise not be identified. Figure 4 demonstrates that in regards to the myocardial wall motion, the post-stress study tended to have a larger degree of motion in all 17-segmental regions as compared to the rest studies. On the other hand, we did not see a similar uniform pattern for the myocardial wall thickening. Nonetheless, it is clear that for myocardial wall motion, and to some extent for myocardial thickening, the standard deviation changes for segmental regions are very similar. However, Figure 7 demonstrates that abnormal myocardial motion and thickening do not always correlate with each other or to those provided by perfusion imaging. It is likely that this is related to the fact that functional changes related to ischemia are likely governed by more complicated relations and the existence of CAD in a particular vessel territory might only exhibit itself in a subset of functional signatures rather than both. Therefore we consider both of these functional signatures, when evaluating the presence of CAD in any particular territory.

The overall lack of sensitivity of TPD for detecting 3VD in our study is similar to a prior study by Christian and colleagues (6). Figure 5 demonstrates the improvement in performance of our hybrid method for detection of 3VD as compared to the traditional TPD method. It should be noted that in our study, a test was considered positive for 3VD detection only if there were abnormalities detected in all three vessel territories, regardless of detection method used. Our proposed hybrid method outperformed the perfusion only diagnostic method by correctly detecting 32 more cases of 3VD out of 109 total patients with 3VD. On the other hand, because our hybrid method did not overrule the TPD positive results, we did not expect any improvements in the overall specificity by employing our method, and this was reflected in the results. These data are consistent with prior studies, which had demonstrated that new reversible regional wall motion abnormality on a post-stress study that was not present during rest is a strong predictor of angiographic severity, and adds incremental value to the perfusion data for assessment of severity (8). Furthermore, Figure 6 demonstrates similar improvement in sensitivity for detection of 2VD, with a similar decline in overall specificity. However, a similar pattern was not seen for detection of 1VD. These findings are similar to a prior study by Sharir et al. (23), who showed that exercise-induced regional wall motion abnormality detected by ^{99m}Tc-sestamibi gated SPECT is a predictor of multi-vessel coronary artery disease.

The overall improvement in detection rate of multi-vessel disease by applying our hybrid method when compared to TPD alone method is evidence that there is incremental value in supplementing myocardial functional information to the traditional perfusion information for diagnosis of multi-vessel disease.

Prior studies have also demonstrated that global functional changes could be utilized for detection of 3VD. A study by Hida and colleagues in 2009 demonstrated that post-adenosine

stress reduction in left ventricular function of ≥ 5% had 60% sensitivity and 77% specificity for detection of multi-vessel CAD (19). However, in our study the accuracy of 3 vessel detection utilizing a drop in EF of ≥ 5% was only 63%, as compared to our hybrid method, which was 69% ($P < 0.004$). A regional approach utilizing our hybrid method along with TPD therefore appears to be a more reasonable approach for detection of multi-vessel disease as compared to the global approach.

There are several limitations related to our study. One of the major limitations is that the functional images are not obtained at the time of maximal stress, but rather up to 45 minutes afterwards. This can possibly decrease the overall sensitivity of our hybrid method. A study by Yoda and colleagues in 2005 demonstrated that the detection of regional wall motion abnormality immediately after exercise provided incremental diagnostic value to the myocardial perfusion images by improving sensitivity for detection of moderate single vessel disease (50–70%) (24). However, other studies have demonstrated that stress-induced myocardial stunning could persist for >1 hour after exercise or adenosine infusion, in patient with severe CAD (7, 25, 26). Another limitation is that the abnormal rest studies will clearly limit the ability to identify new regional wall motion abnormalities on a post-stress sans. In our study, however, cases with myocardial infarctions were excluded. Furthermore, vascular territories defined for myocardial perfusion studies are somewhat imprecise with 2 vessels possibly supplying the same territory, and therefore part of the error of the technique is related possibly to the incorrect territory definition, which cannot be overcome by combination of functional and perfusion analysis.

CONCLUSION

In this study, we presented a novel technique for myocardial surface non-rigid registration to eliminate the polar map indexing disparities between endocardial surfaces of different cardiac cycles and studies (post-stress and rest), and compute motion/thickening changes directly. Our results show the potential value of our proposed method in improving the overall sensitivity for detection of multi-vessel disease as opposed to perfusion only method. Combining regional perfusion measures with regional functional changes appears more accurate for detection of 3VD than the global functional measures utilizing TPD and ejection fraction as a marker of 3VD.

Acknowledgments

This research was supported in part by grant R0HL089765-02S1 from the National Heart, Lung, and Blood Institute/National Institutes of Health (NHLBI/NIH) (PI: Piotr Slomka). Its contents are solely the responsibility of the authors and do not necessarily represent the official views of the NHLBI. We would like to thank Arpine Oganyan for editing and proof-reading the text. Cedars-Sinai Medical Center receives royalties for the licensure of QGS and QPS used in this work, a portion of which is distributed to some of the authors (GG, DB, PK, and PS) of this manuscript.

REFERENCES

1. Klocke FJ, Baird MG, Lorell BH, et al. Committee Members. ACC/AHA/ASNC Guidelines for the Clinical Use of Cardiac Radionuclide Imaging—Executive Summary. Circulation. 2003; 108:1404–1418. [PubMed: 12975245]
2. Sharir T, Ben-Haim S, Merzon K, et al. High-speed myocardial perfusion imaging initial clinical comparison with conventional dual detector anger camera imaging. JACC Cardiovasc Imaging. 2008; 1:156–163. [PubMed: 19356422]
3. Danias PG, Papaioannou GI, Ahlberg AW, et al. Usefulness of electrocardiographic-gated stress technetium-99m sestamibi single-photon emission computed tomography to differentiate ischemic from nonischemic cardiomyopathy. Am J Cardiol. 2004; 94:14–19. [PubMed: 15219501]

4. Slomka PJ, Nishina H, Berman DS, et al. Automatic quantification of myocardial perfusion stress-rest change: a new measure of ischemia. J Nucl Med. 2004; 45:183–191. [PubMed: 14960634]
5. Martin W, Tweddel AC, Hutton I. Balanced triple-vessel disease: enhanced detection by estimated myocardial thallium uptake. Nucl Med Commun. 1992; 13:149–153. [PubMed: 1557213]
6. Christian TF, Miller TD, Bailey KR, et al. Noninvasive identification of severe coronary artery disease using exercise tomographic thallium-201 imaging. Am J Cardiol. 1992; 70:14–20. [PubMed: 1615863]
7. Johnson LL, Verdesca SA, Aude WY, et al. Postischemic stunning can affect left ventricular ejection fraction and regional wall motion on post-stress gated sestamibi tomograms. J Am Coll Cardiol. 1997; 30:1641–1648. [PubMed: 9385888]
8. Emmett L, Iwanochko RM, Freeman MR, et al. Reversible regional wall motion abnormalities on exercise technetium-99m-gated cardiac single photon emission computed tomography predict high-grade angiographic stenoses. J Am Coll Cardiol. 2002; 39:991–998. [PubMed: 11897441]
9. Shirai N, Yamagishi H, Yoshiyama M, et al. Incremental value of assessment of regional wall motion for detection of multivessel coronary artery disease in exercise (201)Tl gated myocardial perfusion imaging. J Nucl Med. 2002; 43:443–450. [PubMed: 11937586]
10. Diamond GA, Forrester JS. Analysis of probability as an aid in the clinical diagnosis of coronary-artery disease. N Engl J Med. 1979; 300:1350–1358. [PubMed: 440357]
11. Slomka PJ, Fish MB, Lorenzo S, et al. Simplified normal limits and automated quantitative assessment for attenuation-corrected myocardial perfusion SPECT. J Nucl Cardiol. 2006; 13:642–651. [PubMed: 16945744]
12. Xu Y, Fish M, Gerlach J, et al. Combined quantitative analysis of attenuation corrected and non-corrected myocardial perfusion SPECT: Method development and clinical validation. J Nucl Cardiol. 2010; 17:591–599. [PubMed: 20387137]
13. Slomka PJ, Berman DS, Xu Y, et al. Fully automated wall motion and thickening scoring system for myocardial perfusion SPECT: Method development and validation in large population. J Nucl Cardiol. 2012 [Epub ahead of print].
14. Germano G, Kavanagh PB, Su HT, et al. Automatic reorientation of three-dimensional, transaxial myocardial perfusion SPECT images. J Nucl Med. 1995; 36:1107–1114. [PubMed: 7769436]
15. Germano G, Kavanagh PB, Slomka PJ, et al. Quantitation in gated perfusion SPECT imaging: the Cedars-Sinai approach. J Nucl Cardiol. 2007; 14:433–454. [PubMed: 17679052]
16. Slomka PJ, Nishina H, Berman DS, et al. Automated quantification of myocardial perfusion SPECT using simplified normal limits. J Nucl Cardiol. 2005; 12:66–77. [PubMed: 15682367]
17. Nakazato R, Tamarappoo BK, Kang X, et al. Quantitative upright-supine high-speed SPECT myocardial perfusion imaging for detection of coronary artery disease: correlation with invasive coronary angiography. J Nucl Med. 2010; 51:1724–1731. [PubMed: 20956478]
18. Berman DS, Kang X, Slomka PJ, et al. Underestimation of extent of ischemia by gated SPECT myocardial perfusion imaging in patients with left main coronary artery disease. J Nucl Cardiol. 2007; 14:521–528. [PubMed: 17679060]
19. Hida S, Chikamori T, Tanaka H, et al. Diagnostic value of left ventricular function after adenosine triphosphate loading and at rest in the detection of multi-vessel coronary artery disease using myocardial perfusion imaging. J Nucl Cardiol. 2009; 16:20–27. [PubMed: 19152125]
20. Lima RSL, Watson DD, Goode AR, et al. Incremental value of combined perfusion and function over perfusion alone by gated SPECT myocardial perfusion imaging for detection of severe three-vessel coronary artery disease. J Am Coll Cardiol. 2003; 42:64–70. [PubMed: 12849661]
21. Yusuf S, Zucker D, Peduzzi P, et al. Effect of coronary artery bypass graft surgery on survival: overview of 10-year results from randomised trials by the Coronary Artery Bypass Graft Surgery Trialists Collaboration. Lancet. 1994; 344:563–570. [PubMed: 7914958]
22. Eagle KA, Guyton RA, Davidoff R, et al. ACC/AHA 2004 guideline update for coronary artery bypass graft surgery: summary article: a report of the American College of Cardiology/American Heart Association Task Force on Practice Guidelines (Committee to Update the 1999 Guidelines for Coronary Artery Bypass Graft Surgery). Circulation. 2004; 110:1168–1176. [PubMed: 15339866]

23. Sharir T, Bacher-Stier C, Dhar S, et al. Identification of severe and extensive coronary artery disease by postexercise regional wall motion abnormalities in Tc-99m sestamibi gated single-photon emission computed tomography. Am J Cardiol. 2000; 86:1171–1175. [PubMed: 11090786]

24. Yoda S, Sato Y, Matsumoto N, et al. Incremental value of regional wall motion analysis immediately after exercise for the detection of single-vessel coronary artery disease: study by separate acquisition, dual-isotope ECG-gated single-photon emission computed tomography. Circ J. 2005; 69:301–305. [PubMed: 15731535]

25. Druz RS, Akinboboye OA, Grimson R, et al. Postischemic stunning after adenosine vasodilator stress. J Nucl Cardiol. 2004; 11:534–541. [PubMed: 15472638]

26. Paul AK, Hasegawa S, Yoshioka J, et al. Exercise-induced stunning continues for at least one hour: evaluation with quantitative gated single-photon emission tomography. Eur J Nucl Med. 1999; 26:410–415. [PubMed: 10199948]

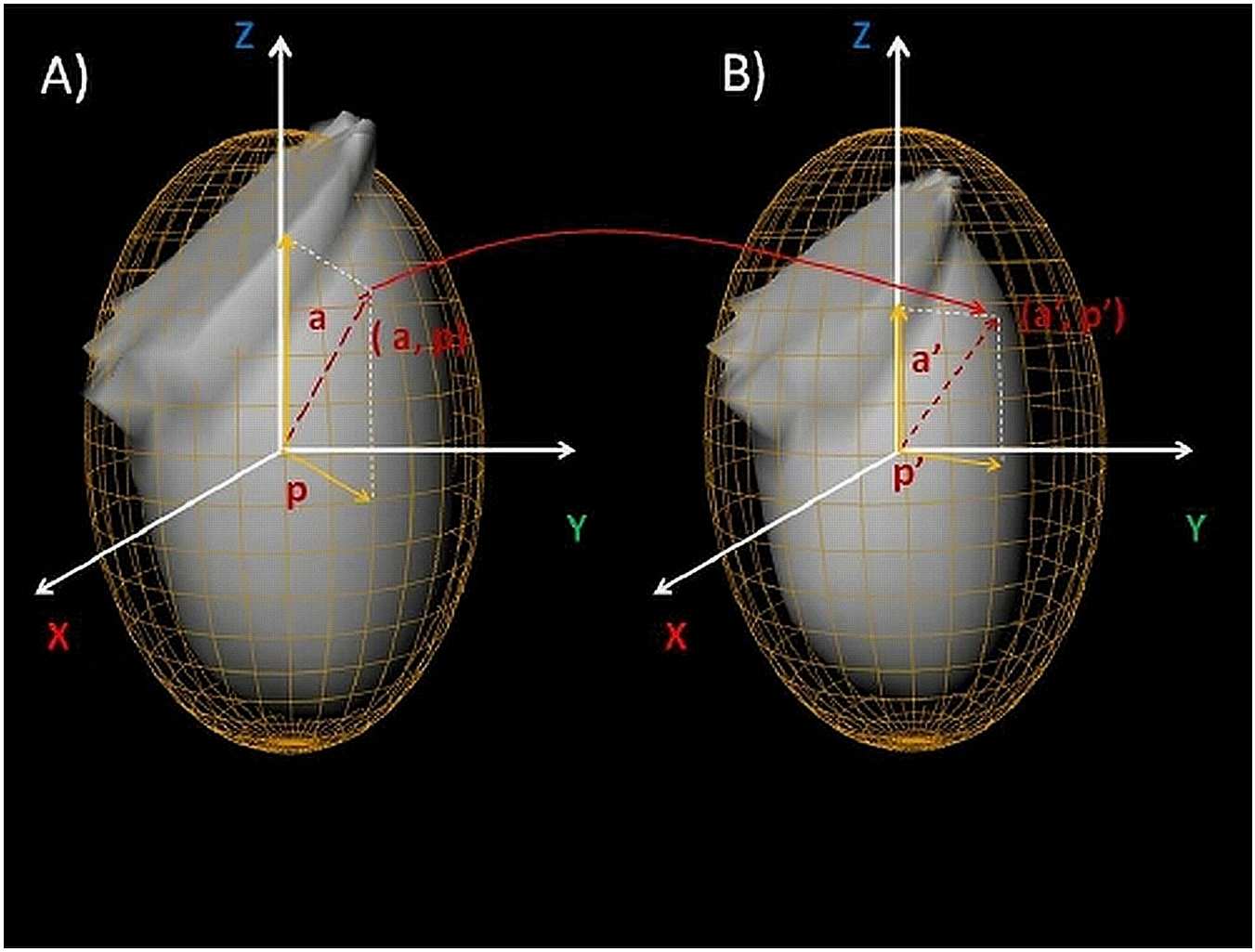

Figure 1.
Segmented endocardial surfaces and their corresponding best ellipsoid fits for Post-Stress ED (A) and Post-Stress ES (B). As a result of independent segmentations of myocardium at ED and ES times, a point indexed by (a, p) at time ED may actually be represented by (a', p') indexes at ES time. This is a potential source of error for myocardial motion and thickening computations, if not compensated by our proposed registration method.

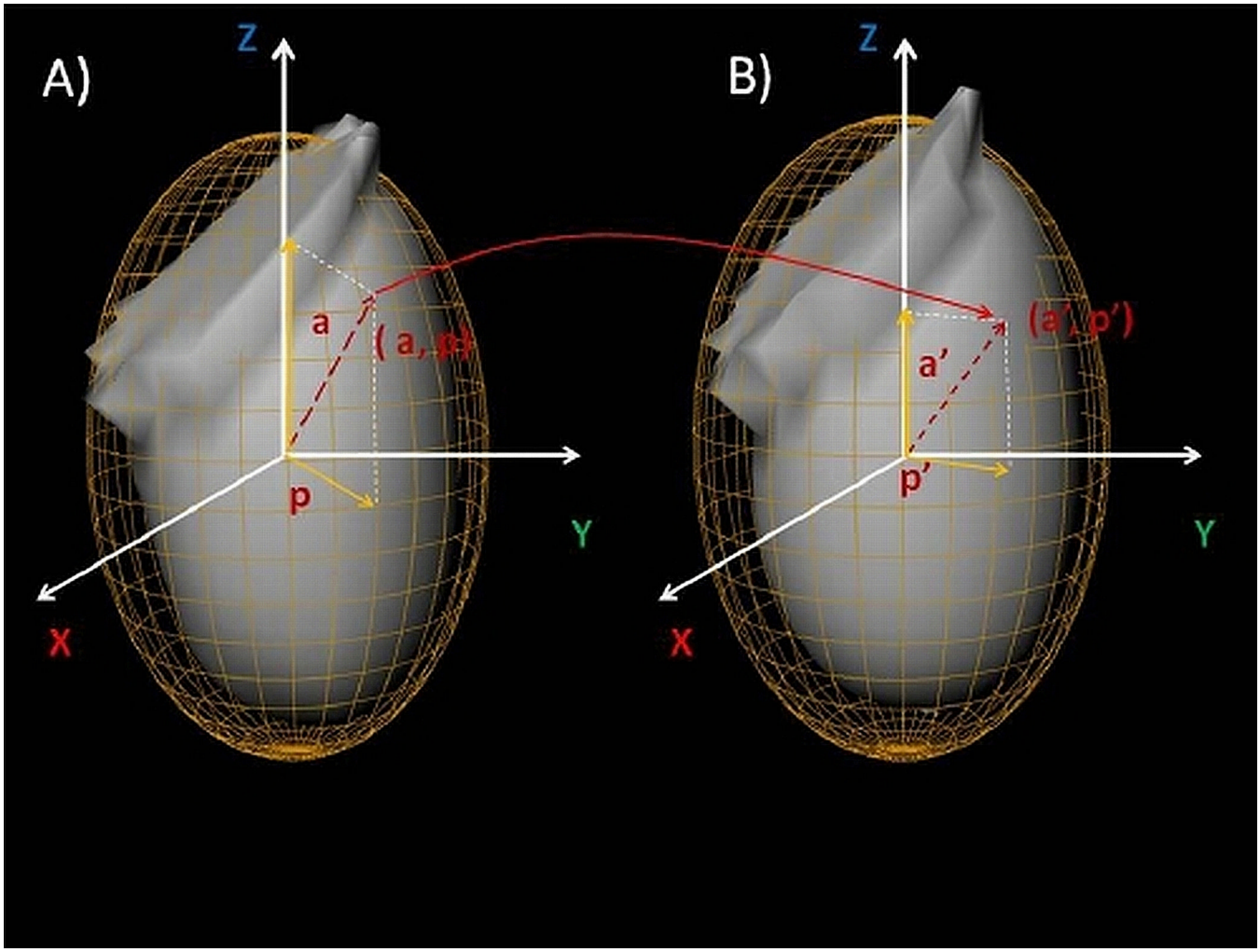

Figure 2.
Endocardial surface segmentation at ED for post-stress (A) and rest (B) studies.

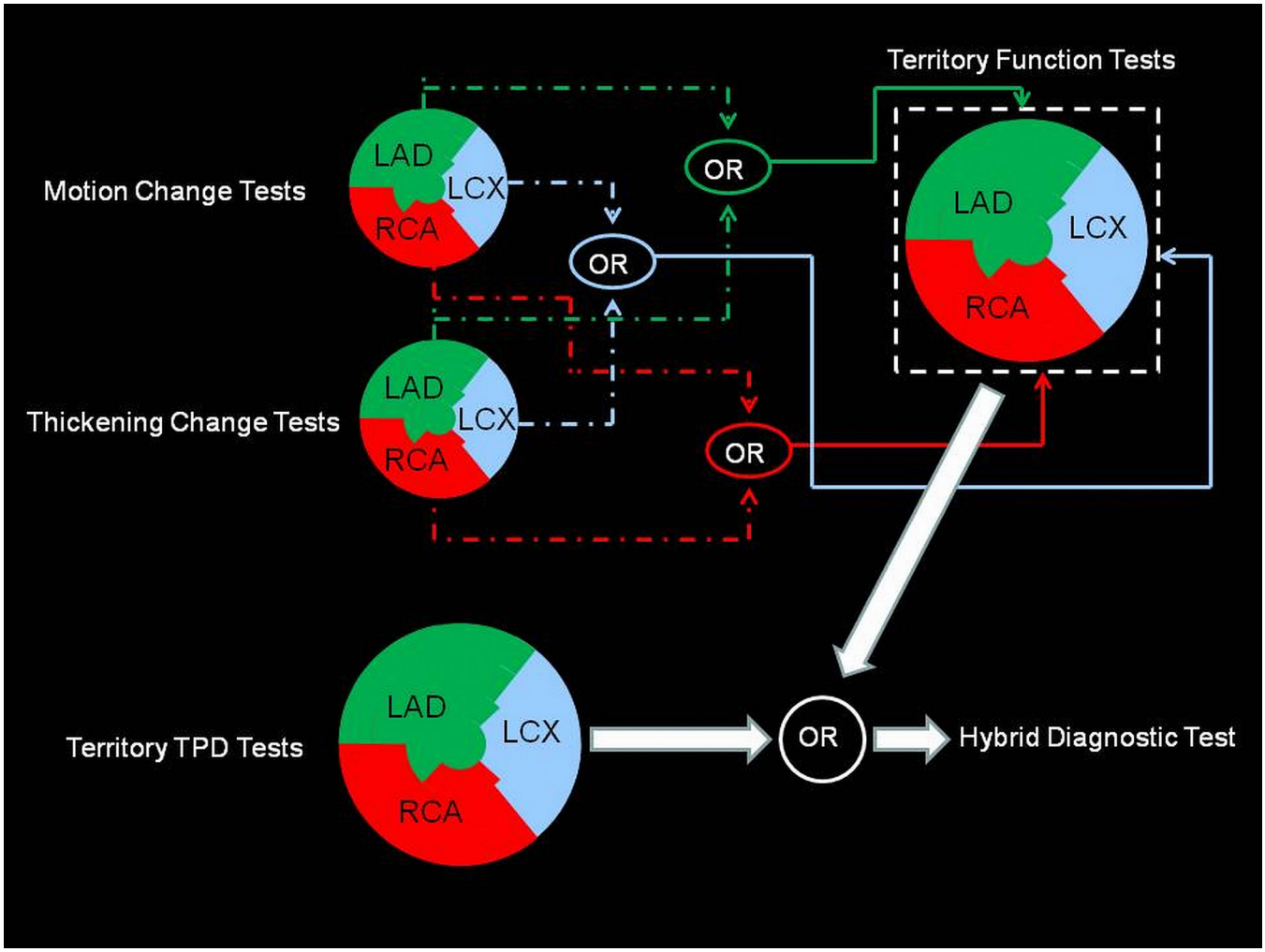

Figure 3.
Schematic of the proposed hybrid system for diagnosis of 3VD condition.

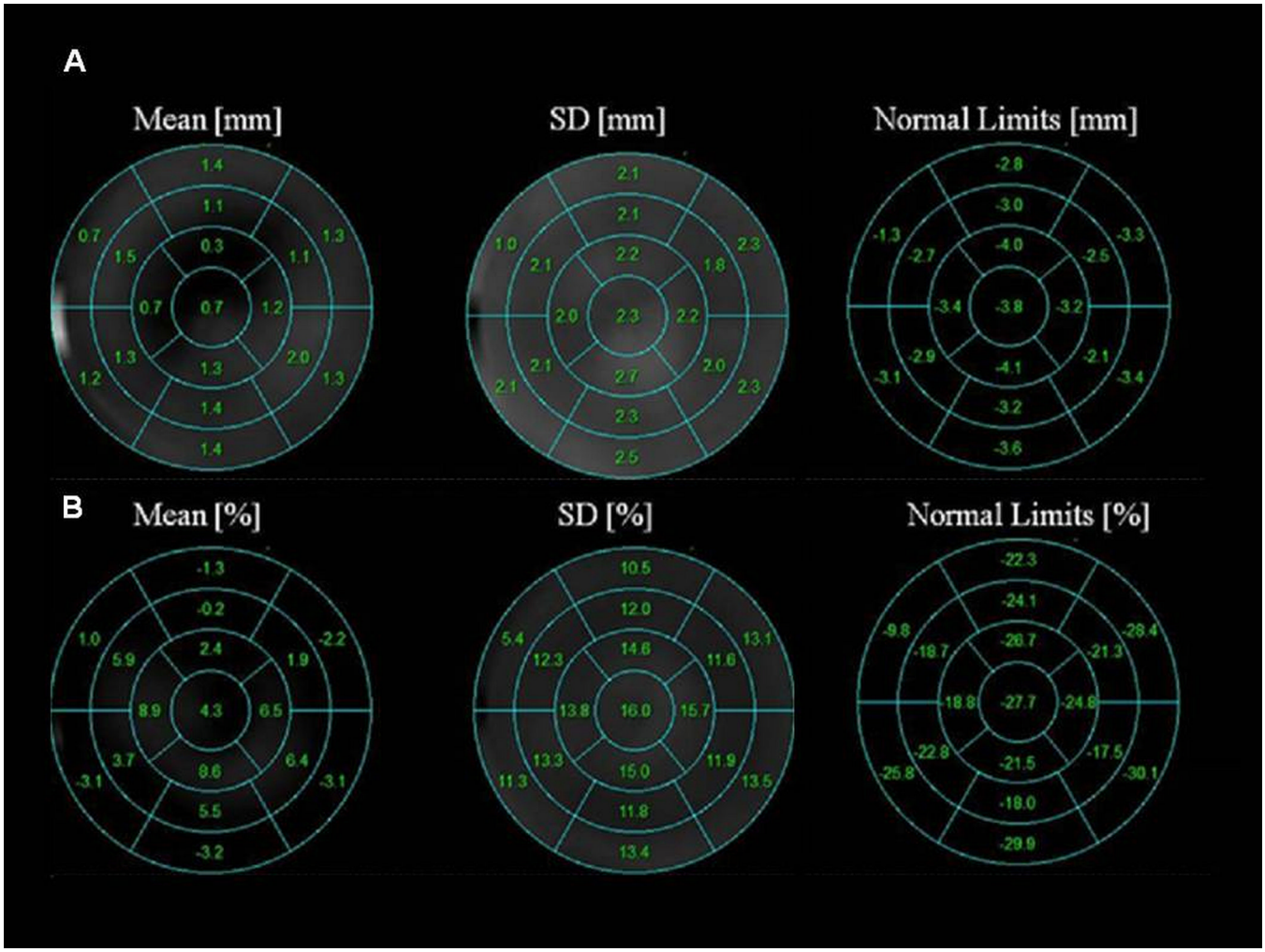

Figure 4.
Segmental normal limits for post-stress-rest motion change (A), Post-stress-rest thickening change (B). The normal limit values are defined as the Mean-2SD for each segment.

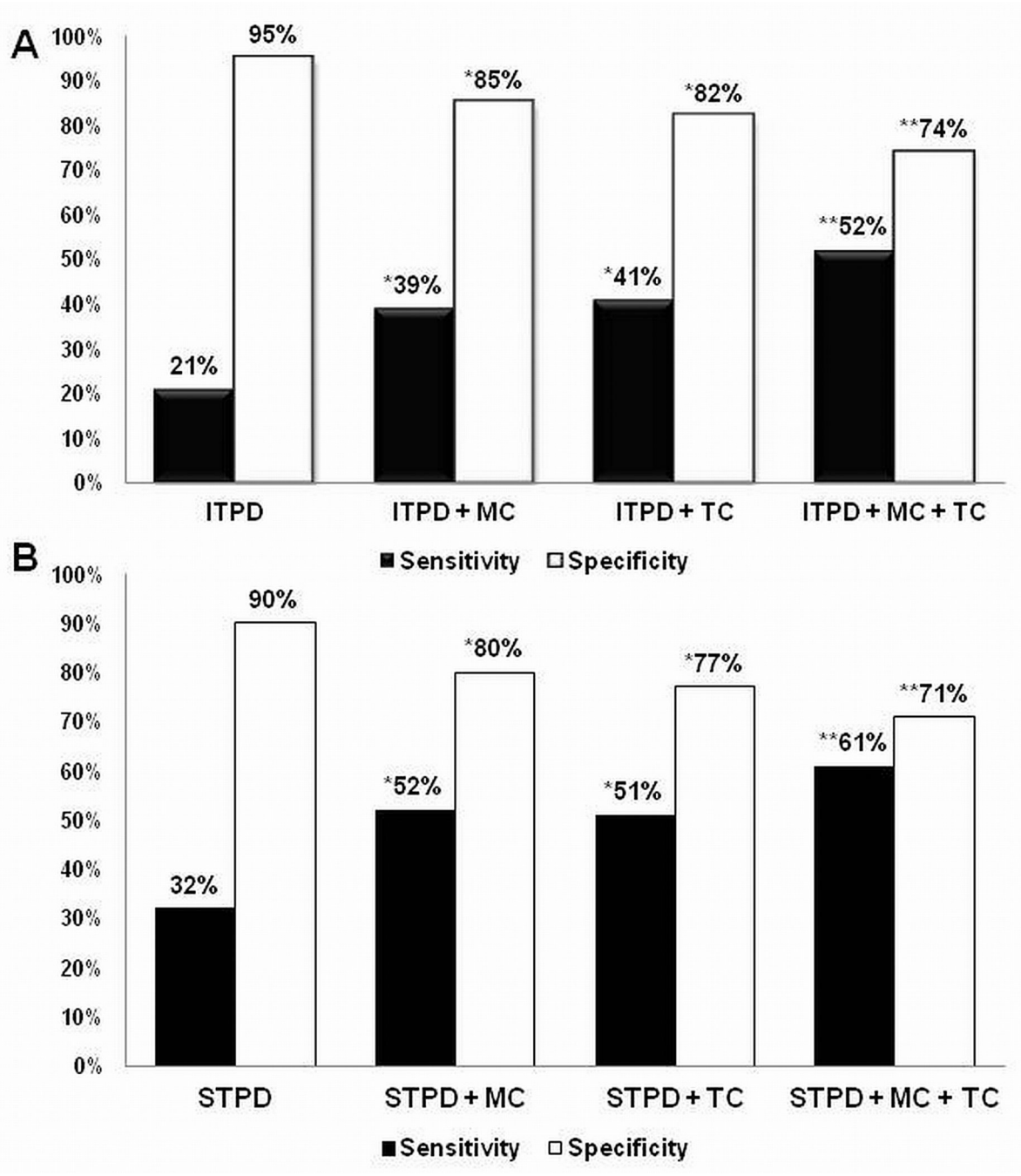

Figure 5.

Three vessel disease detection utilizing Ischemic TPD (A), Stress TPD (B), and our hybrid approach. The abnormality threshold per vessel territory for TPD was set to 2%. MC: Motion Change, TC: Thickening Change, ITPD: Ischemic Total Perfusion Defect, STPD: Stress Total Perfusion Defect. * Sensitivity: $P < 0.0001$, Specificity: $P < 0.0001$. ** Sensitivity: $P < 0.0001$, Specificity: $P < 0.0001$.

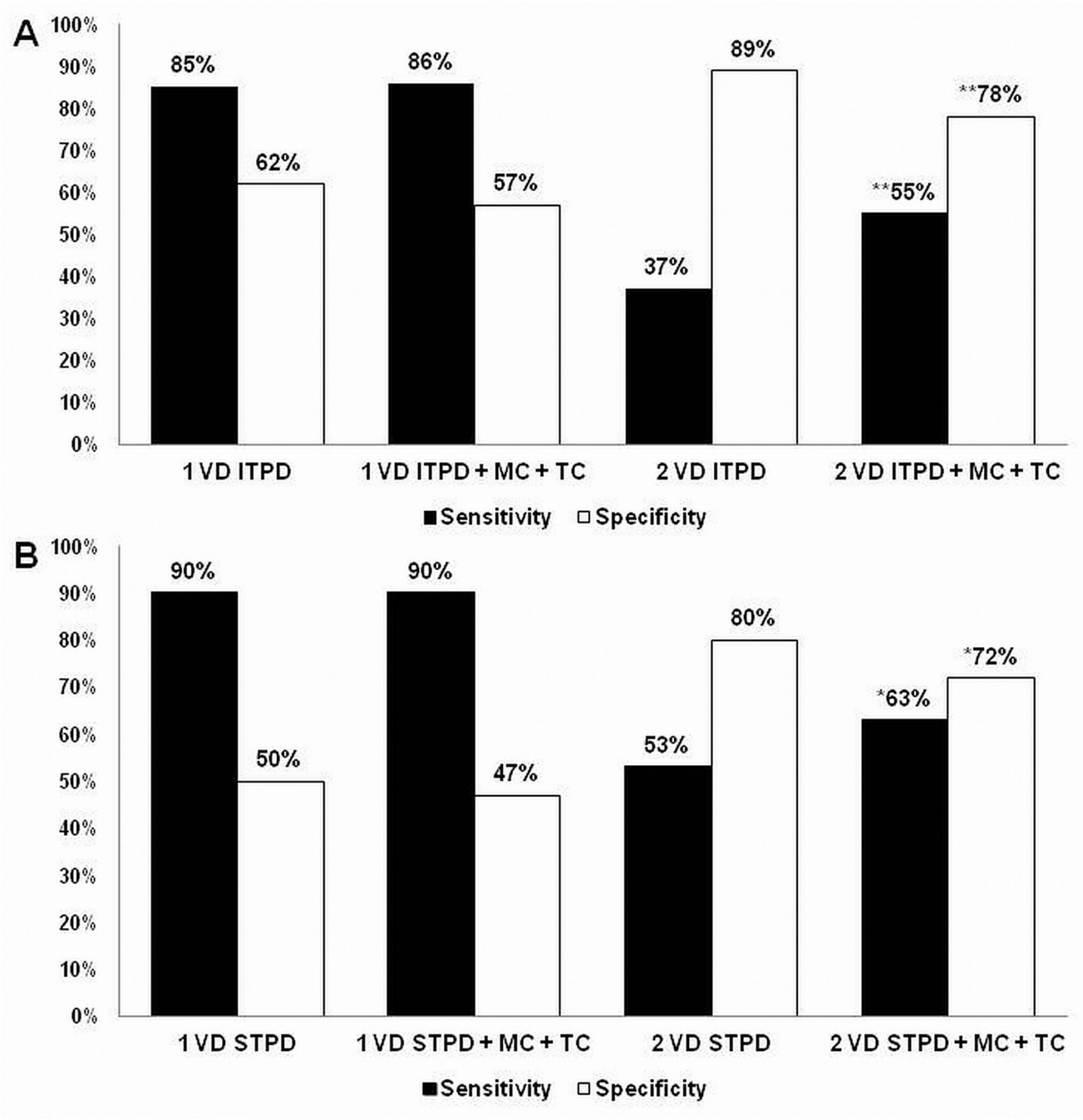

Figure 6.

One-vessel and 2-vessel disease detection utilizing Ischemic TPD (A), Stress TPD (B), and our hybrid approach combining TPD and MTC. The abnormality threshold per vessel territory for TPD was set to 2%. MC + TC: Motion and Thickening Change, ITPD: Ischemic Total Perfusion Defect, STPD: Stress Total Perfusion Defect. * Sensitivity: $P < 0.001$, Specificity: $P < 0.001$. ** Sensitivity: $P < 0.0001$, Specificity: $P < 0.0001$.

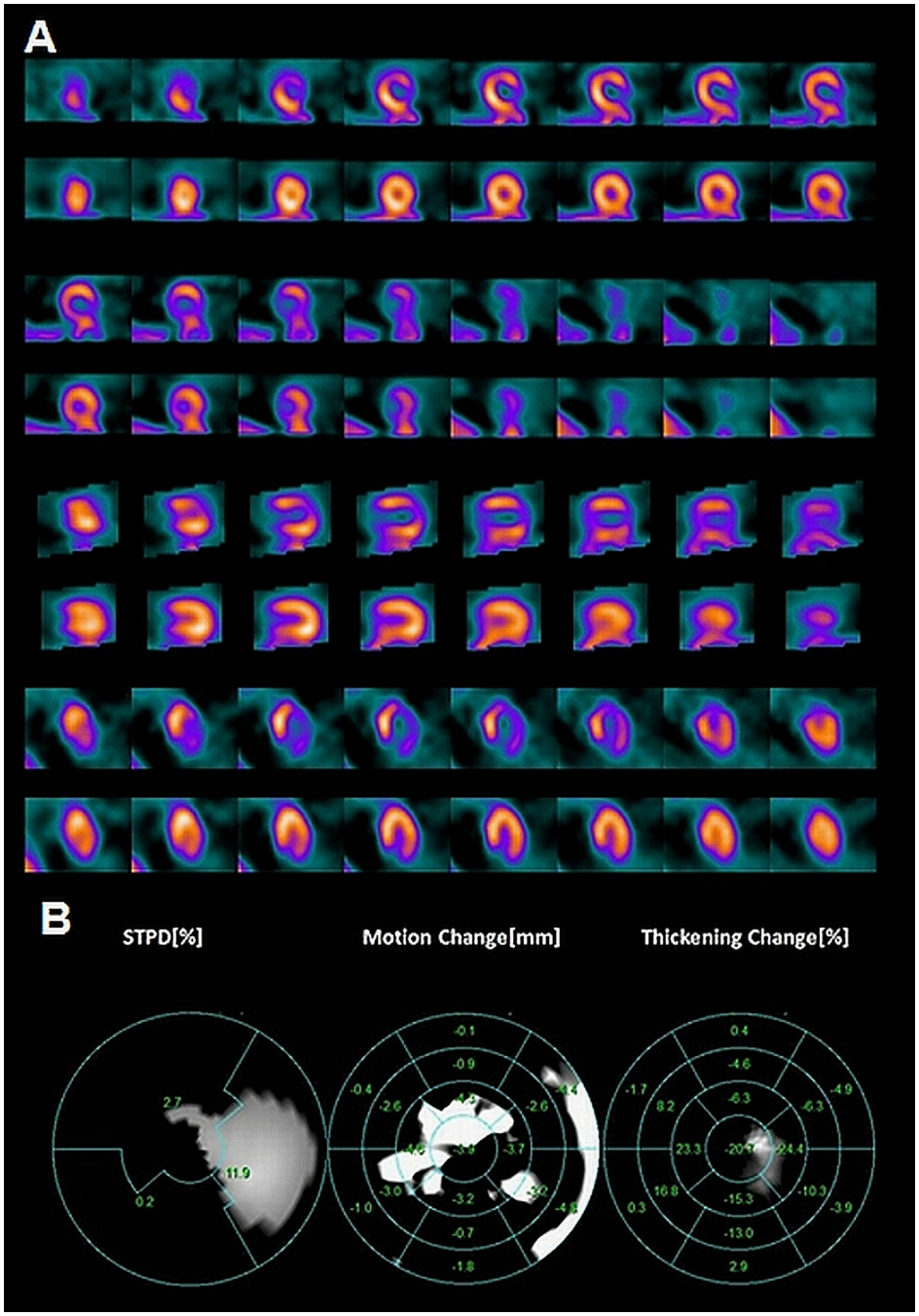

Figure 7.

Stress/Rest myocardial perfusion images of a 53-year-old woman with history of hypertension and hyperlipidemia who underwent ^{99m}Tc-Sestamibi imaging to evaluate chest pain. The stress SPECT images clearly demonstrate a reversible perfusion defect in the left anterior and left circumflex artery territory (A). The motion and thickening change also identify abnormalities in the right coronary artery territory (B). Cardiac catheterization confirmed the presence of 3VD.

TABLE 1

Study group populations and the data acquisition characteristics

	LLK Test / Training	CAD	p-Value
Number of patients	100	623	
Male	30%	56.7%	<0.001
Female	70%	43.3%	<0.001
Age (Years)	52.3 ± 12	64 ± 12	<0.0001
Body Mass Index (BMI)	29 ± 6.7	31 ± 9.6	0.0007
Diabetes	0.0%	27.4%	<0.001
Hypertension	40%	63.5%	<0.001
Hyperlipidemia	40%	51.3%	<0.001
Smoking	23%	23.6%	0.14
Family History	53%	37.4%	0.001
Typical Angina	4.0%	11.4%	<0.001
Dyspnea	11%	11.4%	0.95
8-bin Gated SPECT	98%	62.4%	<0.0001
16-bin Gated SPECT	2%	37.6%	<0.0001
Exercise SPECT	100%	33.1%	<0.0001
Adenosine SPECT	0%	66.9%	<0.0001